Journal of Hazardous Materials 175 (2010) 658–665

Contents lists available at ScienceDirect

Journal of Hazardous Materials

journal homepage: www.elsevier.com/locate/jhazmat

Enhanced photocatalytic discoloration of acid fuchsine wastewater by TiO_2/schorl composite catalyst

Huan-Yan Xu[a,*], Zhuo Zheng[b], Gui-Jie Mao[c]

[a] College of Materials Science and Engineering, Harbin University of Science and Technology, 4#, Linyuan Road, Xiangfang, Harbin 150040, China
[b] College of Materials Science and Engineering, Sichuan University, Chengdu 610064, China
[c] School of Chemistry and Materials Science, Heilongjiang University, Harbin 150080, China

ARTICLE INFO

Article history:
Received 21 August 2009
Received in revised form
30 September 2009
Accepted 14 October 2009
Available online 27 October 2009

Keywords:
TiO_2
Schorl
Composite catalyst
Acid fuchsine
Discoloration

ABSTRACT

The existence of 'electrostatic poles' on the schorl surface encouraged us to apply schorl for a TiO_2 support. TiO_2/schorl composite photocatalyst was prepared and characterized by XRD, SEM and UV/DRS, and their photocatalytic activity was evaluated by discoloration of acid fuchsine (AF). The results indicated that TiO_2 existed in the form of anatase and was well deposited and enwrapped on the schorl surface. The absorption edge of TiO_2/schorl exhibited a slight red shift in the UV/DRS spectra, compared with that of pure TiO_2. The photocatalytic activity of TiO_2/schorl for AF discoloration was higher than that of pure TiO_2. The AF discoloration ratio approached 100% after irradiation time of 12 h. The optimum photocatalyst was found to be that containing 4.76 wt.% of schorl and sintered at 550 °C. The reaction followed pseudo-first-order kinetics, discussed by the Langmuir–Hinshelwood model. Hypotheses were proposed to interpret the mechanism for the enhanced photocatalytic activity of TiO_2/schorl.

1. Introduction

Colored wastewater is released in effluents from textiles, printing, dyeing and food, and poses an increasing environmental danger. In textile industry, it was estimated that 10–15% of the dye was lost during the dyeing process and released as effluents, which constitute threats to environment [1]. Dye pollutants from these industries have a considerable effect on the water environment and are visually unpleasant [2]. Moreover, a variety of organic chemicals are produced during the dyeing process, and some have been shown to be carcinogenic [3]. If these effluent dyestuffs are improperly treated, they will be a threat to all species on earth because the hydrolysis of the pollutants in the wastewater can produce a great deal of toxic products [4]. Techniques for dyeing wastewater decoloration can be grouped into physical, chemical and biological methods [5].

Environmental catalysis performs an essential role in minimizing the emission of toxic compounds and the development of energy saving, residue-free processes [6]. Due to its non-toxic nature, photochemical stability, low cost and complete mineralization of organic and inorganic substrates, TiO_2-based heterogeneous photocatalysis has been considered to be environmentally friendly in the degradation of various organic pollutants [3,7]. TiO_2 works as photocatalysts based on the semiconducting property [8]. The initial process for TiO_2 photocatalysis is the generation of electron–hole pairs in the semiconductor particles. When a photon of light, of sufficient energy ($E \geq E_{bg}$) strikes a TiO_2 particle, the energy of the photon is absorbed and used to promote an electron (e^-) from the valence band to the conduction band. This movement of an electron leaves a hole (h^+) in the valence band. These species (h^+ and e^-) generated by the absorption of light, can either recombine or they migrate to the surface of the TiO_2 particle where they can react with other species at the interface. The holes can directly oxidize organic species adsorbed onto the TiO_2 particle or can give rise to hydroxyl radicals ($^\bullet OH$) by reacting with water or OH^-. These highly reactive hydroxyl radicals then attack organic compounds present at or near the surface [9]. However, the pure TiO_2 exhibits spectral response only in UV region [10]. Thereby, there are two main obstacles for the practical application of TiO_2 photocatalyst: low quantum efficiency and restriction to short wavelength excitation [11,12]. Several attempts of modification methods have been made, such as single metal element doping [4,8,9,11–13], single non-metal element doping [14], combination of metals and/or non-metals doping [10,15] and composite semiconductors [16,17], to extend the absorption spectrum to visible light, to slow down the recombination rate of the electron–hole pairs and to enhance the interfacial charge transfer efficiency [13]. Moreover, with the decreasing size of the TiO_2 nanoparticles, the photocatalytic activ-

* Corresponding author. Tel.: +86 451 8639 2956; fax: +86 451 8639 2522.
E-mail address: xhy7587@yahoo.com.cn (H.-Y. Xu).

0304-3894/$ – see front matter © 2009 Elsevier B.V. All rights reserved.
doi:10.1016/j.jhazmat.2009.10.059

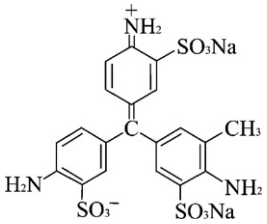

Fig. 1. Chemical structure of acid fuchsine.

ity will be greatly improved, owing to the surface effect and quanta size effect [18]. But, it will bring about a new problem that fine TiO_2 powder is difficultly separated from the aqueous phase after use. Several methods have been explored to solve this problem, such as preparation of TiO_2 film [12,13] and TiO_2 nano-fiber [18] or immobilization of TiO_2 powder onto supports like Al_2O_3 [19], clay [20], zeolite [2,7,21] and activated carbon [3,22,23]. However, the immobilization usually decreases the overall photoactivity of TiO_2 [19].

Although ionic doping in the structure of the TiO_2 crystal can prevent the electron–hole recombination, which is advantage for the improvement of the quantum efficiency, some photogenerated positive holes may be recombination centers, if the accumulated negative charges are not consumed or not further transferred out of the metal particles. External electric field is applied to drive these accumulated electrons to improve the photocatalytic activity of TiO_2. This process is described as photo-electro-catalytic process [24], whose efficiency is much higher than that of the single photocatalytic process [25]. Schorl is one kind of minerals of tourmaline groups. It has unique characteristics of pyroelectricity and piezoelectricity [26]. It has been confirmed that the spontaneous (or the permanent) 'electrostatic poles' exist on the surface of the tourmaline crystals at room temperature [27], and this property encourages us to approach to application of tourmaline for a TiO_2 support. Hence, in our present study, TiO_2 loaded on schorl was prepared by sol–gel method and the composite samples were characterized by X-ray diffraction (XRD), scanning electron microscopy (SEM) and diffuse reflection spectra (UV/DRS). The photocatalytic activity of the composite samples was evaluated using acid fuchsine (AF) as the model pollutant under UV irradiation.

2. Experimental

2.1. Materials

Powdered particles of schorl, using as the support for TiO_2, were purchased from Wuhua-Tianbao Mining Resources Co. Ltd., Inner-Mongolia, China. The physical properties and chemical compositions have been discussed in our previous work [28]. Analytical-grade tetrabutyltitanate (TBOT) was used as the precursor of TiO_2; analytical-grade reagents of ethanol, acetic acid, and deionized water were used to prepare the composite catalysts. Analytical-grade dye of acid fuchsine (AF) was selected as the model pollutant; its chemical structure is shown in Fig. 1.

2.2. Preparation of catalysts

Before use, the powdered particles of schorl were pretreated with HCl (1 mol/L) at room temperature for 24 h, washed with deionized water repeatedly, till pH value of the lotion up to neutrality, and then dried at 80 °C in oven. Sol–gel method was used to prepare the catalysts. In stirred condition, the mixed solvent of TBOT/ethanol/acetic acid, at a volumetric ratio of 1:2:3, was dropwise added to the schorl suspension that had been stirred for 20 min in adequate amount of ethanol solvent. The mixture was stirred at 60 °C for 3 h in air, and then $NH_3{\cdot}H_2O$ was added to adjust the pH to 8. Subsequently, the solvent was removed by filtration and the resultant solid was dried in oven at 100 °C for 5 h. Finally, the prepared sample was sintered at different temperatures for 3 h, respectively. After ground, the powdered sample of TiO2/schorl composite catalyst was obtained. As comparison, the pure TiO_2 sample was also prepared using the same procedure except for the addition of schorl.

2.3. Characterization of catalysts

The crystal structure of catalysts was determined by XRD. Measurements were carried out on a D/MAX-3B X-ray diffractometer with Cu-K_α radiation at 30 mA and 40 kV, over the 2θ range of 10–80°. The crystal morphology of catalysts was observed by SEM. Measurements were made on a FEISirion200 SEM instrument using a digital imaging process. UV/DRS was employed to analyze changes in band energy of catalysts. The UV/DRS spectra in the range of 200–800 nm were recorded on a Lambda900 UV–vis spectrometer equipped with an integral sphere using $BaSO_4$ as a reference. The BET specific surface area of catalysts was obtained from nitrogen adsorption–desorption data and measured using a ST-08 surface area analyzer at liquid nitrogen temperature.

2.4. Photocatalytic experiments

The photocatalytic activity of the composite catalysts was estimated by using AF and halogen tungsten lamp as the model pollutant and irradiation source, respectively. The photocatalytic discoloration of AF was conducted in a 200 mL glass reactor at room temperature. The 15 W ZSZ15-40 UV lamp, with predominant UV radiation at a wavelength of 365 nm, was located at about 15 cm above the solution. A stock solution containing AF (1000 mg/L) was prepared using deionized water, subsequently diluted to the required concentrations for the experimental work. The concentration of AF was maintained at 100 mg/L for all the photocatalytic discoloration. 100 mL of the AF solution and 0.5 g of the photocatalyst were placed in the reactor before irradiation. At regular time intervals of irradiation, 2 mL of the samples was collected from the reactor for measurements of AF concentrations, using a 721-type UV–vis spectrophotometer. The discoloration ratio, i.e. the removal degree of color at the λ_{max} of the AF solution (545 nm) was calculated using $D_R\ (\%) = (C_0 - C_t)/C_0 \times 100$, where C_0 is the initial concentration of the AF wastewater and C_t the concentration at irradiation time t. In order to evaluate the adsorption of AF on the photocatalysts, experiments were run under the same condition but without UV irradiation. The measurement of AF concentrations and calculation of AF adsorption ratios were conducted using the same method mentioned previously. In order to check the reproducibility of the results, random tests were done for different experimental conditions.

3. Results and discussion

3.1. Photocatalysts characterization

The composite photocatalysts with 0, 0.99, 2.91, 4.76, 6.54 wt.% of schorl using as the TiO_2 support were prepared at 550 °C, labeled as TiO_2, TS099-550, TS291-550, TS476-550, and TS654-550, respectively. At the same time, the sintering temperatures of 350, 450, 650, and 750 °C were adopted to prepare the composite photocatalysts with 4.76 wt.% of schorl, and the samples were denoted as TS476-350, TS476-450, TS476-650, and TS476-750, respectively. Fig. 2 shows the XRD patterns of the composite catalysts containing different amounts of schorl. Six distinctive TiO_2 peaks can be found

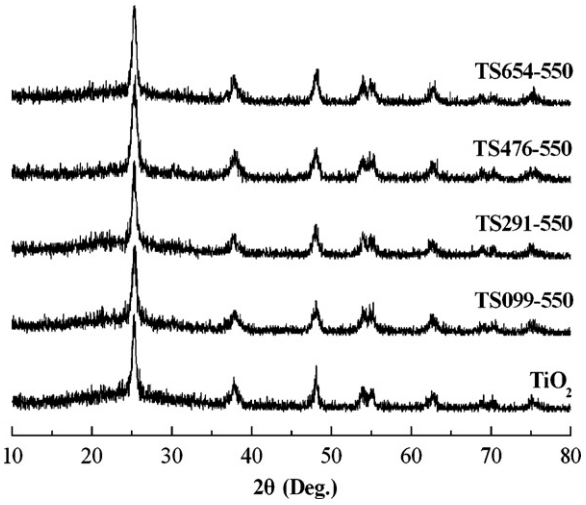

Fig. 2. XRD patterns of the composite catalysts containing different amounts of schorl.

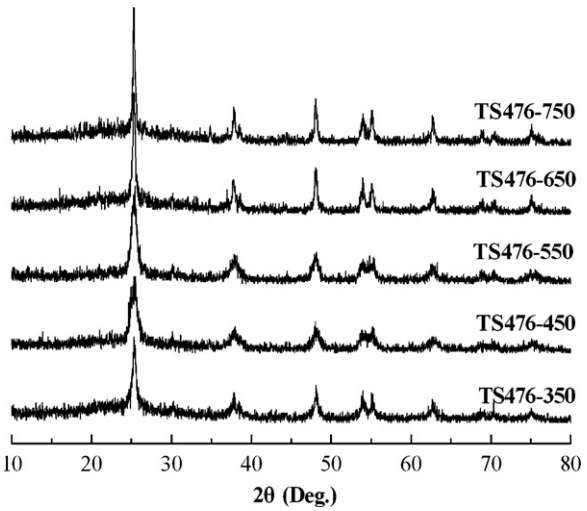

Fig. 3. XRD patterns of the composite catalysts sintered at different temperatures.

at 2θ of 25.28°, 37.93°, 48.38°, 53.89°, 55.29° and 64.17°, corresponding to the crystal planes of (1 0 1), (0 0 4), (2 0 0), (1 0 5), (2 1 1), and (2 0 4) of the anatase phase of TiO_2 (JCPDS 78-2486), respectively. This result indicates that TiO_2 exists in the form of anatase phase. As expected, no rutile phase can be found in all samples, which is beneficial to photocatalytic activity of the composite catalysts, owing to higher photocatalytic activity of anatase than that of rutile [18]. No XRD peaks of schorl can be observed in the patterns. This might be due to the fact that the content of schorl is so low that it cannot be detected by XRD. Similar results have been found and reported by Song's group, when they loaded 10 wt.% tourmaline mineral onto TiO_2 [29]. Based on the XRD results, the crystal size of TiO_2 was calculated by the Scherrer formula, i.e. $D = K\lambda/\beta\cos\theta$, where D is the crystallite size in nm, β is the full-width-at-half-maximum for the peak of (101) plane, λ is the wavelength of the X-ray radiation (0.15418 nm), and K is the Scherrer constant, assumed to be 0.9 [16,22]. The TiO_2 crystallite sizes for TiO_2, TS099-550, TS291-550, TS476-550, and TS654-550 are listed in Table 1. The data clearly reveal that, compared with pure TiO_2, the addition of schorl can make the TiO_2 crystallite size smaller, which confirms that the electrostatic field on the schorl surface can strongly affect the nucleation and growth of TiO_2 [30] and matches the result reported by Song's group [29]. Moreover, the results of the surface area of these catalysts (Table 1) indicate that the surface area increases with the increasing amount of schorl. This means that, in the composite catalysts, TiO_2 particles are restricted to agglomerate and well dispersed by depositing on the surface of schorl particles. The more the amount of schorl is, the better the dispersion of TiO_2 particles is; whereas, pure TiO_2 particles are easier to agglomerate than that of deposited ones [22]. The effects of sintering temperature on the XRD patterns of the composite photocatalysts are shown in Fig. 3. Similarly, the composite photocatalysts are dominated by anatase, and the phase of rutile and schorl cannot be found in all samples. It is well known that TiO_2 exists in three different crystalline habits: anatase (tetragonal), brookite (orthorhombic) and rutile (tetragonal). Rutile is the stable form, whereas anatase and brookite are metastable and are readily transformed to rutile when heated [31]. The anatase–rutile transformation does not have a transition temperature because there is no phase equilibria involved. For this reason, the anatase–rutile transition does not take place at a defined temperature and was observed at temperatures between 400 and 1000 °C, strongly dependent on the impurity content in TiO_2 and the reaction atmosphere [32]. Previously reported literatures for the anatase–rutile transformation reveal various informations. For example, some researchers considered that the rutile phase of TiO_2 appeared at 600 °C or 700 °C, and formed completely at 900 °C [33,34]. Contrary to that, the presence of two phases (anatase and rutile) after heat treatment up to 900 °C was observed by Stojanović's group [35]; Liu and Chen found that, in S-doped TiO_2 photocatalyst, the phase transformation of anatase to rutile started at 800 °C, which is much higher than naked TiO_2 [36]; when the double salt $(NH_4)_2TiO(SO_4)_2$ was decomposed in the static air to prepare TiO_2, rutile occurred at 800 °C or above [37]; and, when anatase TiO_2 powders were prepared by an alcohothermal method using tetra-n-butyl titanate as a precursor, even calcination at 800 °C for 4 h, the main crystal phase was still anatase, and small peaks of rutile phase began to appear [38]. From these samples, it can be concluded that the anatase–rutile transforma-

Table 1
TiO_2 crystallite size, surface area, AF adsorption capacity and adsorption ratio for different catalysts.

Sample	TiO_2 crystallite size (nm)	Surface area (m^2/g)	Adsorption capacity for AF (mg/g)	AF adsorption ratio (%)
Sample containing different amounts of schorl				
TiO_2	49.2	14.37	2.37	11.86
TS099-550	33.2	33.81	2.56	12.81
TS291-550	39.3	41.95	2.85	14.26
TS476-550	33.2	59.47	8.89	36.43
TS654-550	33.2	64.38	9.23	40.15
Sample sintered at different temperatures				
TS476-350	50.2	18.11	2.40	11.98
TS476-450	28.8	46.89	3.89	19.47
TS476-550	33.2	59.47	8.89	36.43
TS476-650	67.3	13.05	2.06	10.32
TS476-750	67.3	11.81	1.85	9.26

tion occurs at a wider range of temperature, owing to different experimental conditions. In this work, it may be the addition of schorl that inhibits phase transformation of TiO_2 from anatase to rutile. Accordantly with our results, when 10 wt.% tourmaline mineral was loaded onto TiO_2, rutile phase appeared at 800 °C [29]. The TiO_2 crystallite sizes for TS476-350, TS476-450, TS476-550, TS476-650, and TS476-750 are listed in Table 1. The results reveal that an increase in sintering temperature beyond 350 °C results in an intensity enhancement and narrowing of (1 0 1) peak, indicating a progressive growth of crystallites [24]. Nevertheless, according to the general scheme for TiO_2 crystallization processes, TS476-350 is very exceptional, with larger TiO_2 crystallite size and narrower (1 0 1) peak than TS476-450 and TS476-550. Possible reason for this phenomenon is advanced according to anatase crystallization kinetics model. It can be assumed that a thin layer of the product propagates fast from the reacting interface into the center of a particle and that the rate-determined process is controlled by diffusion or phase-boundary reaction [35]. At 350 °C, the electrostatic effect of schorl may exceed the thermal effect of temperature and the former can accelerate the diffusion process during anatase crystallization, so anatase can be well crystallized at lower temperature leading to the conclusion that the whole process is determined by a rather fast rate, exhibiting larger TiO_2 crystallite size and narrower (1 0 1) peak. With sintering temperature increasing beyond 350 °C (350–450 °C), the thermal effect of temperature possibly increases and gradually exceeds the electrostatic effect of schorl, and then a new equilibrium is established between the thermal and electrostatic effect. Now, the system is predominant by the thermal effect, which might drive anatase crystallites fragmentize, rearrange and even recrystallize, resulting in smaller TiO_2 crystallite size and broader (1 0 1) peak of TS476-450 than those of TS476-350. Continuing increasing the sintering temperature (450–750 °C) can make a progressive growth of anatase crystallites driven by the thermal effect, resulting in the order of TiO_2 crystallite size being TS476-450 < TS476-550 < TS476-650 < TS476-750.

The surface morphology of the pure TiO_2 and composite photocatalysts was examined by SEM and Fig. 4 shows representative SEM micrographs. Observed from Fig. 4(a), it becomes clear that, for the pure TiO_2, the TiO_2 particles present irregular shapes and they desultorily aggregate together. However, for the composite photocatalysts, it can be observed that the particles of TiO_2 are well deposited and enwrapped on the surface of each schorl particle (Fig. 4(b) and (c)). And, it is found that the agglomerate of the TiO_2 particles on the schorl surface in the composite is much compacter than that in pure TiO_2. Possible reason advanced for this is that the agglomerating TiO_2 particles on the surface of schorl in the composite are affected by the strong electrostatic adsorption due to the function of the electrostatic field on the schorl surface, which makes the TiO_2 particles assemble more compactly and be tightly fixed on the schorl surface. Furthermore, the observed size of most TiO_2 particles is larger than that calculated from XRD, because the latter is the size of a single crystallite; whereas, the particles shown in the SEM micrographs are the agglomerates of many TiO_2 crystallites [22].

The UV/DRS spectra of the photocatalysts using different amounts of schorl as TiO_2 support were measured in the region of 200–800 nm and are depicted in Fig. 5. The spectra are quite similar each other in shape; whereas, the thresholds of band gap transition for TiO_2 supported on schorl show a slight red shift, compared with that for pure TiO_2. The band gap energy, E_g, of the sample can be calculated from Eq. (1) [39]:

$$E_g = \frac{1239.8}{\lambda} \quad (1)$$

where E_g is the band gap (eV) of the sample and λ (nm) is the wavelength of the onset of the spectrum. According to Sun's method

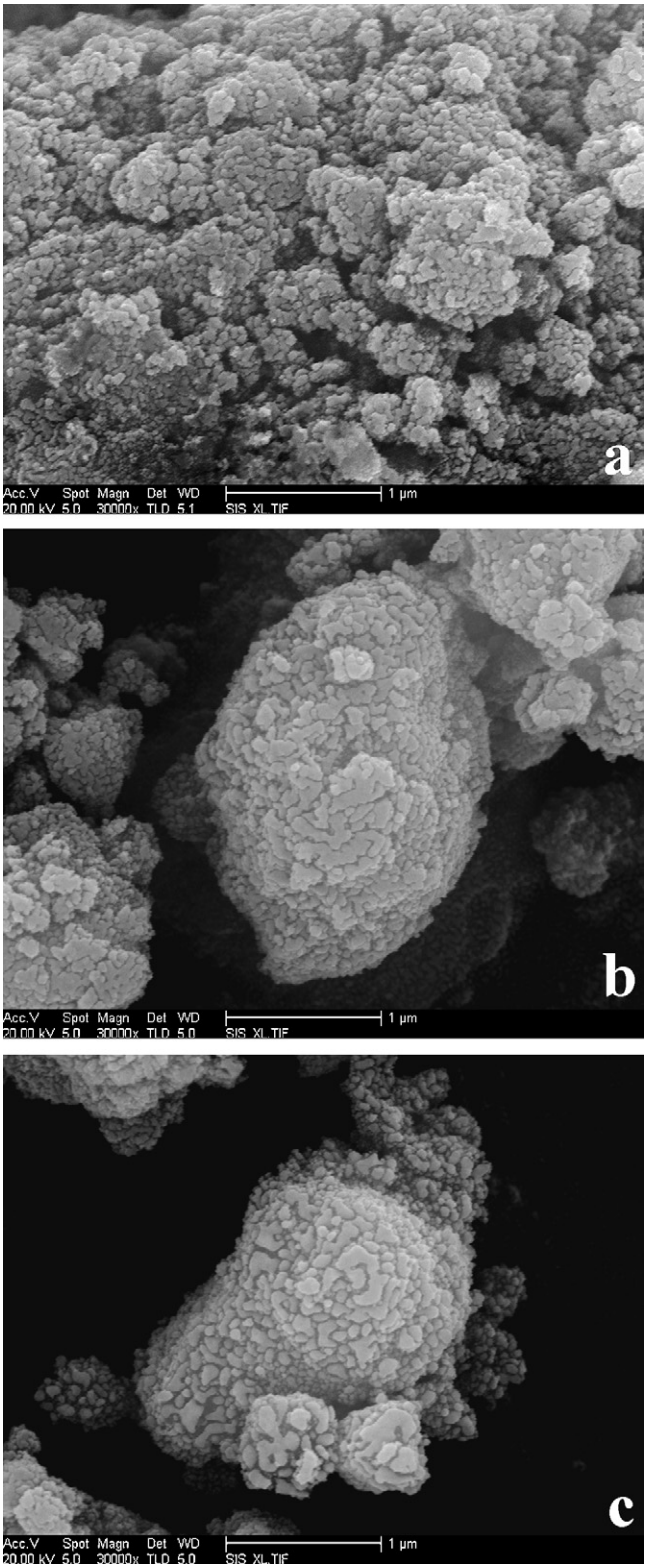

Fig. 4. Representative SEM micrographs for (a) the pure TiO_2 sample and the composite photocatylysts (b) TS476-550 and (c) TS654-550.

[40], the absorption threshold of pure TiO_2 is 344 nm, and its band gap is calculated as 3.60 eV. There is no significant difference in absorption threshold and band gap among the three TiO_2/schorl composite photocatalysts, with λ of about 349 nm and E_g 3.55 eV. It clearly exhibits that the addition of schorl can make the absorption edge shift to longer wavelengths, corresponding to a decrease in the

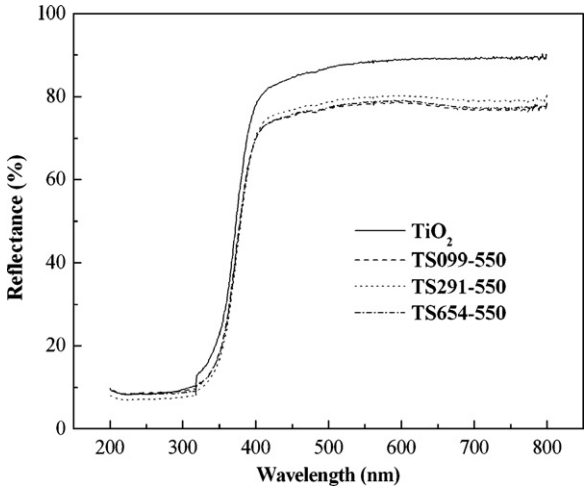

Fig. 5. UV/DRS spectra of TiO_2 and TiO_2/schorl.

band gap energy. This may be due to the fact that charges transition from the TiO_2 valence band or conduction band and their migrations to the surface of the TiO_2 particles can be enhanced by the electrostatic field on the surface of schorl and the band gap energy in the TiO_2/schorl composite catalyst is lower than that of the pure TiO_2. Furthermore, all these composite photocatalysts show much enhanced absorption in the visible light region (400–800 nm). This is because the addition of schorl can extend the light absorption region of TiO_2 and weak light absorption occurs in this region for TiO_2/schorl composites. Another possible reason put forward to interpret this phenomenon may be due to the black characteristic of schorl, similar to the result of a TiO_2/AC catalyst reported by Liu's group [41].

3.2. Photocatalytic performance

To evaluate the photocatalytic activity of the composite catalyst, photocatalytic discoloration of AF was carried out under UV irradiation. The AF discoloration experiments were executed at chosen reaction parameters as previously mentioned in Section 2.4, and the results are presented in Fig. 6. Keeping all other experimental parameters constant, the composite catalysts containing different wt.% of schorl as TiO_2 supports were employed to understand their impact on the AF discoloration, as depicted in Fig. 6(a). The data clearly indicate that the AF discoloration ratio by the TiO_2/schorl composite catalyst is higher than that by the pure TiO_2, which suggests that schorl can improve the photocatalytic activity of TiO_2. When the pure TiO_2 is used as photocatalyst, 12 h are required for the AF discoloration ratio approaching 85%; whereas, only 3 h are needed for the similar result, when TS476-550 or TS654-550 is used as catalyst. After 12-h discoloration, the AF discoloration ratio can come up to 100% and the carmine color of AF in aqueous solution is invisible. It is generally accepted that adsorption is critical in heterogeneous photocatalytic oxidation processes [2]. Thus, the adsorption of AF onto the different catalysts was also tested in this work. In the dark adsorption experiments, the catalysts were used only as absorbents, and the adsorption process was kept in dark for 12 h. It was found that the maximum adsorption reached within 2 h and no further significant change occurred, illustrating establishment of a substrate adsorption/desorption equilibrium. The saturated adsorption capacity of AF for different catalysts and corresponding AF adsorption ratio are listed in Table 1. The results suggest that, besides photocatalysis, adsorption also can contribute to the AF discoloration and the difference in the adsorption capacity is mainly caused by the surface area of

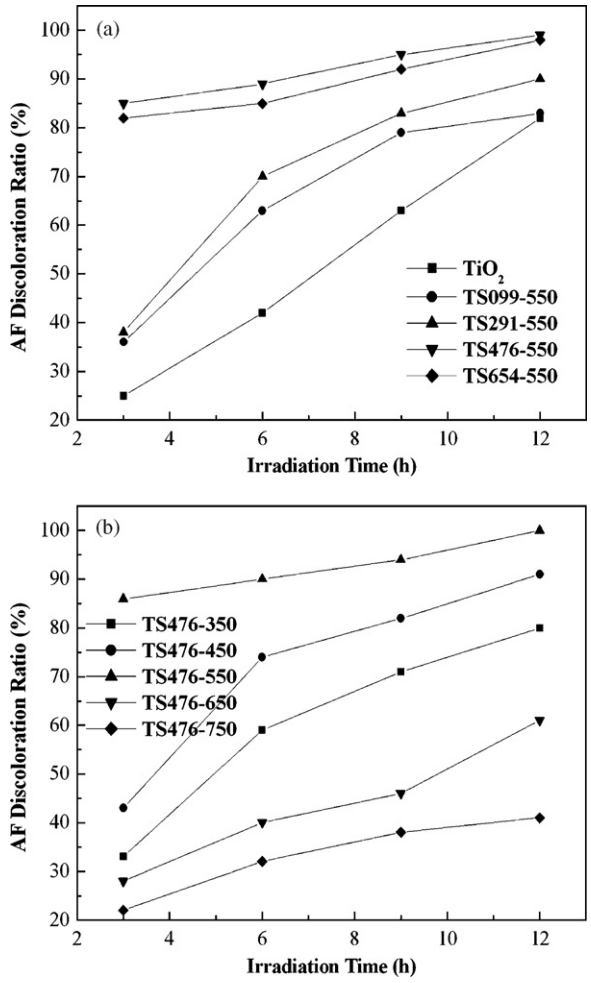

Fig. 6. Photocatalytic discoloration of AF over the TiO_2/schorl composite catalyst (a) containing different schorl contents and (b) sintered at different temperatures.

the catalysts. So, the AF discoloration is related to a synergistic effect of adsorption and photocatalysis. For TS476-550 or TS654-550, the occurrence of faster discoloration of AF in the first three hours may be ascribed to the fact that, on one hand, their AF adsorption ratios are much higher than those of the other three catalysts; on the other hand, for a chemical reaction (except for zero order reaction), the higher the concentration is, the faster the reaction rate is [22], and their photocatalytic reaction rates are improved because of higher concentration of AF adsorbed on TS476-550 or TS654-550. Subsequently, as AF molecules are decomposed by the photocatalysis, the concentration of AF decreases in the solution, so that the adsorbed AF molecules are desorbed from the catalysts and new adsorption/desorption equilibrium is established, which can reduce the AF adsorption capacity and photocatalytic reaction rate. Thus, as a whole, the increase in AF discoloration ratio for TS476-550 or TS654-550 becomes very slow after 3-h discoloration. Furthermore, in this study, the optimum photocatalyst for the photocatalytic discoloration of AF is found to be TS476-550, which implies 4.76 in wt.% is the preferable content of schorl in the composite photocatalyst for the rapid transfer of the photogenerated electrons from TiO_2 semiconductor to the interface of TiO_2/schorl and tight adsorption of the electrons on the anode of schorl. The non-linear relationship between discoloration or removal ratios and support contents has been observed and discussed in many studies [2,7,19]. And, similar results have been found in the decomposition of 2-chlorophenol by tourmaline loaded on TiO_2 [29] and the degradation of methyl orange by SiO_2/TiO_2 doping with tour-

maline [42]. In our study, possible reasons put forward to interpret this phenomenon are that, on one hand, more than 4.76% of schorl in the composite catalyst might make the electrostatic field on the surface of schorl adsorb or disturb each other, as a whole, resulting in the reduction of the electrostatic strength; on the other hand, less than 4.76% of schorl in the composite catalyst might make relatively less amounts of 'electrostatic poles', which could reduce chances for the photogenerated electron migrating from TiO_2 to the interface of TiO_2/schorl, leading to the increase in recombination of the electrons and holes. The effects of the sintering temperatures on the performance of the TiO_2/schorl catalysts in the AF discoloration are shown in Fig. 6(b). For the composite catalyst TS476-550, only 3 h are needed for the AF discoloration ratio approaching 85%; whereas, after 12-h discoloration, only 40% of the AF discoloration ratio can be achieved by TS476-750. The reason for faster discoloration of AF in the first three hours for TS476-550 has been discussed above. From the results, optimum temperature is found to be 550 °C in this study. The relationship between the AF discoloration ratio and the sintering temperature of the composite catalyst is attributed to the dependency of the catalyst surface area on the sintering temperature. As listed in Table 1, the surface areas are 17.11, 46.89, 50.47, 13.05, and 11.81 m^2/g for TS476-350, TS476-450, TS476-550, TS476-650 and TS476-750, respectively. It is clear that the sequence of increase in the AF discoloration ratio is consistent with that of increase in the catalyst surface area. The larger the catalyst surface area is, the higher the AF adsorption capacity is (see Table 1). Moreover, larger catalyst surface area can increase the number of the active sites to enhance the absorption of photons [7].

The relationship between photocatalytic reaction rate and the concentration of dye obeys the Langmuir–Hinshelwood (L–H) kinetic model [2]:

$$r = \frac{dC}{dt} = \frac{kKC}{1 + KC} \tag{2}$$

where r is the reaction rate, C the dye concentration at any time t, k the reaction rate constant, and K is the constant of adsorption equilibrium of the dye onto the photocatalyst particle. This equation can be integrated between the limits: $C = C_0$ at $t = 0$ and $C = C$ at $t = t$. The integrated expression is given by:

$$\ln\left(\frac{C_0}{C}\right) + K(C_0 - C) = kKt \tag{3}$$

where C_0 is the initial concentration of the dye and t is the irradiation time. When the concentration C is relatively high, $>5 \times 10^{-3}$ mol/L, namely $KC \gg 1$, the L–H kinetics can be approximated to be of pseudo-zero-order; whereas, When the concentration C is highly diluted, $<10^{-3}$ mol/L, namely $KC \ll 1$, the L–H kinetics can be approximated to be of pseudo-first-order [43]. In this study, the AF concentration at any time is $\leq 1.71 \times 10^{-4}$ mol/L, thus, Eq. (2) can be approximated to a pseudo-first-order kinetics:

$$\ln\left(\frac{C_0}{C}\right) = kKt = k_a t \tag{4}$$

In order to check whether the reaction rate, in this study, accords with a first-order reaction, curves between $\ln(C/C_0)$ versus irradiation time t are plotted (Fig. 7) under different conditions. As shown in Fig. 7(a), obtained for the composite catalyst containing different schorl contents, a good linear relationship between $\ln(C/C_0)$ and t can be observed, indicating that our experimental data are in agreement with Eq. (4). And, the same situation exists in Fig. 7(b), for the composite catalyst sintered at different temperatures. This finding suggests that the photocatalytic discoloration of AF over the TiO_2/schorl catalyst follows a pseudo-first-order kinetic equation.

The following description is widely accepted as the mechanism for photocatalytic degradation of organic pollutants over TiO_2 system [44]:

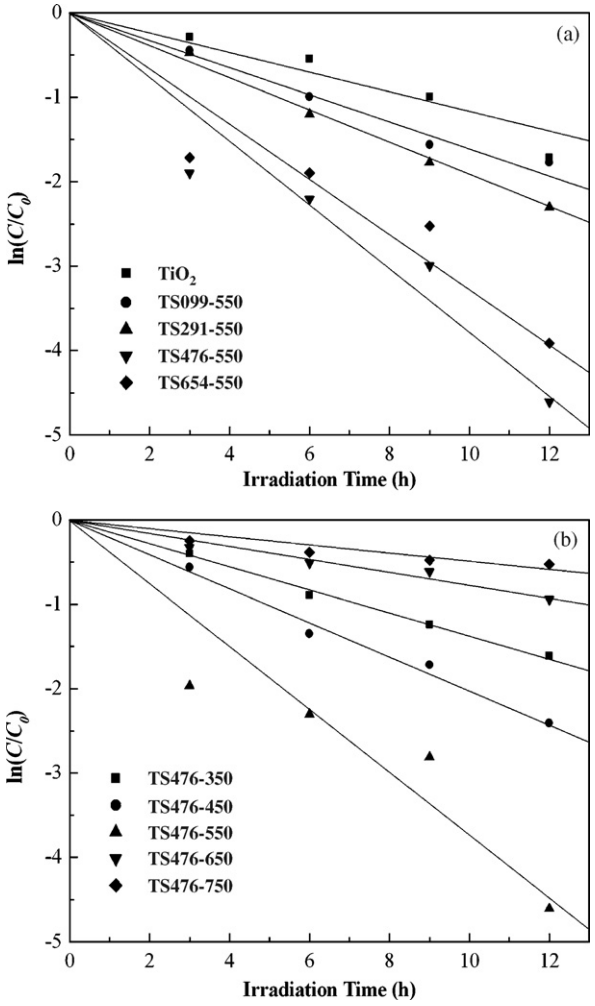

Fig. 7. Relationship between $\ln(C/C_0)$ and irradiation time of the AF discoloration over the TiO_2/schorl composite catalyst (a) containing different schorl contents and (b) sintered at different temperatures.

$$TiO_2 + h\nu \rightarrow TiO_2(e^- + h^+) \tag{5}$$

$$TiO_2(h^+) + OH^- \rightarrow TiO_2 + {}^\bullet OH \tag{6}$$

$$TiO_2(h^+) + H_2O \rightarrow TiO_2 + H^+ + {}^\bullet OH \tag{7}$$

$$TiO_2(e^-) + O_2 \rightarrow TiO_2 + {}^\bullet O_2^- \tag{8}$$

$${}^\bullet O_2^- + H^+ \rightarrow {}^\bullet HO_2 \tag{9}$$

$$TiO_2(e^-) + H^+ + {}^\bullet O_2^- \rightarrow HO_2^- \tag{10}$$

$$HO_2^- + H^+ \rightarrow H_2O_2 \tag{11}$$

When TiO_2 semiconductor is irradiated by light with energy equal to or greater than its band gap energy, an electron can be excited from the valence band to the conduction band and the electron–hole pairs are thus generated (Eq. (5)). $^\bullet OH$ is formed mainly by the oxidation of OH^- or H_2O via photogenerated holes (Eqs. (6) and (7)), and $^\bullet OH$ is the chief oxidant for photocatalytic degradation in wastewater treatment [19]. Unfortunately, the holes show high affinities for the electrons and the high degree of the recombination of the electron–hole pairs is a major limiting factor controlling the photocatalytic efficiency. The unique characteristics of schorl are the existence of the spontaneous (or the permanent) 'electrostatic poles' on its surface. When the TiO_2/schorl composite catalyst is illuminated by UV irradiation, the electron–hole pairs

are generated and the photogenerated electrons will be adsorbed tightly on the anode of schorl, owing to its strong electrostatic field, which suppresses the recombination of the electron–hole pairs. Thus, more hydroxyl radicals are probably formed through the reaction of OH^- or H_2O with more photogenerated holes. Consequently, the TiO_2/schorl composite catalyst shows higher photocatalytic activity than the pure TiO_2. Furthermore, judging from Eq. (8), it can be aware of that oxygen acts primarily as an efficient electron trap, preventing the recombination of the photogenerated electron–hole pairs. Due to the synergistic effect of far infrared, polarity and electrostatic field produced by schorl, the existence of schorl can increase the content of oxygen solved in water [42], which can promote the reaction in Eq. (8). This is one of the possible reasons for higher photocatalytic activity of the TiO_2/schorl composite catalyst. Another possible reason is that, apart from the existence of the 'electrostatic poles', schorl is a natural mineral bearing iron ion, which can catalyze H_2O_2 [28]. In the route of the photocatalytic reaction, H_2O_2 can be formed in Eq. (11) and then catalyzed by schorl to produce $^{\bullet}OH$.

In conclusion, the photocatalytic discoloration of AF can be enhanced by the TiO_2/schorl composite catalyst, attributed to the reasons explained above. As a novel photo-electro-catalytic process, the TiO_2/schorl composite catalyst can eliminate the application of an external electric field. Thus, schorl is utilized and energy is saved.

4. Conclusions

To enhance the photocatalytic activity of TiO_2, the TiO_2/schorl composite catalysts containing different amounts of schorl and sintered at different temperatures were prepared using sol–gel method in this study. TiO_2 existed in the form of anatase phase and the phase of rutile and schorl could not be found in all samples. The particles of TiO_2 agglomerated into clusters and were well dispersed and enwrapped on the surface of schorl. The onset of band gap transition for the TiO_2 sample supported on schorl shown a slight red shift in the UV/DRS spectra, compared with that for the pure TiO_2. The photocatalytic activity of the TiO_2/schorl composite catalyst for the AF discoloration under UV irradiation was higher than that of the pure TiO_2. After 12-h discoloration, the AF discoloration ratio could come up to 100% and the carmine color of AF in aqueous solution was invisible. The optimum photocatalyst for the discoloration of AF was found to be TS476-550. The photocatalytic discoloration of AF over the TiO_2/schorl catalyst followed a pseudo-first-order kinetic equation. Hypotheses were proposed to interpret the mechanism for the enhancement of the photocatalytic activity, including that electrostatic field on the surface of schorl could inhabit the recombination of the photogenerated electron–hole pairs, schorl could increase the content of oxygen solved in water to consume the photogenerated electrons and iron ion existing in schorl could catalyze H_2O_2 formed in the route of the TiO_2 photocatalytic reaction to produce more hydroxyl radicals. As a novel photo-electro-catalytic process, the TiO_2/schorl composite catalyst would have a good prospect in industrial application.

Acknowledgements

This work was supported by a grant from Scientific Foundation of Heilongjiang Office of Education (no. 11531035) and Natural Science Foundation of Heilongjiang Province, China (no. E200906).

References

[1] Y.M. Dong, K. He, B. Zhao, Y. Yin, L. Yin, A.M. Zhang, Catalytic ozonation of azo dye active brilliant red X-3B in water with natural mineral brucite, Catal. Commun. 8 (2007) 1599–1603.
[2] C.-C. Wang, C.-K. Lee, M.-D. Lyu, L.-C. Juang, Photocatalytic degradation of C.I. Basic Violet 10 using TiO_2 catalysts supported by Y zeolite: an investigation of the effects of operational parameters, Dyes Pigments 76 (2008) 817–824.
[3] R. Yuan, R. Guan, W. Shen, J. Zheng, Photocatalytic degradation of methylene blue by a combination of TiO_2 and activated carbon fibers, J. Colloid Interface Sci. 282 (2005) 87–91.
[4] J. Wang, W. Sun, Z. Zhang, Z. Jiang, X. Wang, R. Xu, R. Li, X. Zhang, Preparation of Fe-doped mixed crystal TiO_2 catalyst and investigation of its sonocatalytic activity during degradation of azo fuchsine under ultrasonic irradiation, J. Colloid Interface Sci. 320 (2008) 202–209.
[5] Y.M. Slokar, A.M. Le Marechal, Methods of decoloration of textile wastewater, Dyes Pigments 37 (1998) 335–356.
[6] J.G. Carriazo, M.A. Centeno, J.A. Odriozola, S. Moreno, R. Molina, Effect of Fe and Ce on Al-pillared bentonite and their performance in catalytic oxidation reactions, Appl. Catal. A: Gen. 317 (2007) 120–128.
[7] M. Mahalakshmi, S.V. Priya, B. Arabindoo, M. Palanichamy, V. Murugesan, Photocatalytic degradation of aqueous propoxur solution using TiO_2 and Hβzeolite-supported TiO_2, J. Hazard. Mater. 161 (2009) 336–343.
[8] D. Masih, H. Yoshitake, Y. Izumi, Photo-oxidation of ethanol on mesoporous vanadium-titanium oxide catalysts and the relation to vanadium (IV) and (V) sites, Appl. Catal. A: Gen. 325 (2007) 276–282.
[9] H.M. Coleman, K. Chiang, R. Amal, Effects of Ag and Pt on photocatalytic degradation of endocrine disrupting chemicals in water, Chem. Eng. J. 113 (2005) 65–72.
[10] Y. Huo, Y. Jin, J. Zhu, H. Li, Highly active $TiO_{2-x-y}N_xF_y$ visible photocatalyst prepared under supercritical conditions in NH_4F/EtOH fluid, Appl. Catal. B: Environ. 89 (2009) 543–550.
[11] X.-G. Hou, F.-H. Hao, B. Fan, X.-N. Gu, X.-Y. Wu, A.-D. Liu, Modification of TiO_2 photocatalytic films by V^+ ion implantation, Nucl. Instrum. Methods Phys. Res. B 243 (2006) 99–102.
[12] C.-C. Chan, C.-C. Chang, W.-C. Hsu, S.-K. Wang, J. Lin, Photocatalytic activities of Pd-loaded mesoporous TiO_2 thin films, Chem. Eng. J. 152 (2009) 492–497.
[13] M. Bellardita, M. Addamo, A. Di Paola, L. Palmisano, Photocatalytic behaviour of metal-loaded TiO_2 aqueous dispersions and films, Chem. Phys. 339 (2007) 94–103.
[14] Y.Q. Wang, X.J. Yu, D.Z. Sun, Synthesis, characterization, and photocatalytic activity of $TiO_{2-x}N_x$ nanocatalyst, J. Hazard. Mater. 144 (2007) 328–333.
[15] T. Morikawa, T. Ohwaki, K. Suzuki, S. Moribe, S. Tero-Kubota, Visible-light-induced photocatalytic oxidation of carboxylic acids and aldehydes over N-doped TiO_2 loaded with Fe, Cu or Pt, Appl. Catal. B: Environ. 83 (2008) 56–62.
[16] R.-F. Chen, C.-X. Zhang, J. Deng, G.-Q. Song, Preparation and photocatalytic activity of Cu^{2+}-doped TiO_2/SiO_2, Int. J. Miner. Metall. Mater. 16 (2009) 220–225.
[17] X.Z. Li, F.B. Li, C.L. Yang, W.K. Ge, Photocatalytic activity of WO_x-TiO_2 under visible light irradiation, J. Photochem. Photobiol. A: Chem. 141 (2001) 209–217.
[18] W. Zhou, Y. Zhou, S. Tang, Formation of TiO_2 nano-fiber doped with Gd^{3+} and its photocatalytic activity, Mater. Lett. 59 (2005) 3115–3118.
[19] L.-C. Chen, F.-R. Tsai, C.-M. Huang, Photocatalytic decolorization of methyl orange in aqueous medium of TiO_2 and Ag-TiO_2 immobilized on α-Al_2O_3, J. Photochem. Photobiol. A: Chem. 170 (2005) 7–14.
[20] V. Belessi, D. Lambropoulou, I. Konstantinou, A. Katsoulidis, P. Pomonis, D. Petridis, T. Albanis, Structure and photocatalytic performance of TiO_2/clay nanocomposites for the degradation of dimethachlor, Appl. Catal. B: Environ. 73 (2007) 292–299.
[21] M.V.P. Sharma, V. Durgakumari, M. Subrahmanyam, Solar photocatalytic degradation of isoproturon over TiO_2/H-MOR composite systems, J. Hazard. Mater. 160 (2008) 568–575.
[22] X. Wang, Y. Liu, Z. Hu, Y. Chen, W. Liu, G. Zhao, Degradation of methyl orange by composite photocatalysts nano-TiO_2 immobilized on activated carbons of different porosities, J. Hazard. Mater. 169 (2009) 1061–1067.
[23] X. Zhang, L. Lei, Effect of preparation methods on the structure and catalytic performance of TiO_2/AC photocatalysts, J. Hazard. Mater. 153 (2008) 827–833.
[24] B. Xie, Y. Xiong, R. Chen, J. Chen, P. Cai, Catalytic activities of Pd-TiO_2 film towards the oxidation of formic acid, Catal. Commun. 6 (2005) 699–704.
[25] Y. Su, X. Zhang, M. Zhou, S. Han, L. Lei, Preparation of high efficient photoelectrode of N-F-codoped TiO_2 nanotubes, J. Photochem. Photobiol. A: Chem. 194 (2008) 152–160.
[26] K. Shigenobu, T. Matsumura, T. Nakamura, H. Ishii, Y. Nishi, Ecological uses of tourmaline, in: Proceedings First International Symposium on Environmentally Conscious Design and Inverse Manufacturing, 1–3 February, Tokyo, Japan, 1999, pp. 912–915.
[27] T. Nakamura, T. Kubo, Tourmaline group crystals reaction with water, Ferroelectrics 137 (1992) 13–31.
[28] H.Y. Xu, M. Prasad, Y. Liu, Schorl: a novel catalyst in mineral-catalyzed Fenton-like system for dyeing wastewater discoloration, J. Hazard. Mater. 165 (2009) 1186–1192.
[29] S.H. Song, M. Kang, Decomposition of 2-chlorophenol using a tourmaline photocatalytic system, J. Ind. Eng. Chem. 14 (2008) 785–791.
[30] J.-S. Liang, J.-P. Meng, G.-C. Liang, Y.-W. Feng, Y. Ding, Preparation, photocatalytic activity of composite films containing clustered TiO_2 particles and mineral tourmaline powders, Trans. Nonferrous Metals Soc. China 16 (2006) s542–s546.
[31] A. Di Paola, G. Cufalo, M. Addamo, M. Bellardita, R. Campostrini, M. Ischia, R. Ceccato, L. Palmisano, Photocatalytic activity of nanocrystalline TiO_2 (brookite, rutile and brookite-based) powders prepared by thermohydrolysis of $TiCl_4$ in

aqueous chloride solutions, Colloids Surf. A: Physicochem. Eng. Aspects 317 (2008) 366–376.
[32] F.C. Gennari, D.M. Pasquevich, Kinetics of the anatase-rutile transformation in TiO_2 in the presence of Fe_2O_3, J. Mater. Sci. 33 (1998) 1571–1578.
[33] H.F. Jiang, H.Y. Song, Z.X. Zhou, X.Q. Liu, G.Y. Meng, Characterization of LiF-doped TiO_2 and its photocatalytic activity for decomposition of trichloromethane, Mater. Res. Bull. 43 (2008) 3037–3046.
[34] S.T. Oh, J.S. Choi, H.S. Lee, L.H. Lu, H.H. Kwon, I.K. Song, J.J. Kim, H.I. Lee, H_2O-controlled synthesis of TiO_2 with nanosized channel structure through in situ esterification and its application to photocatalytic oxidation, J. Mol. Catal. A: Chem. 267 (2007) 112–119.
[35] B.D. Stojanović, Z.V. Marinković, G.O. Branković, E. Fidančevska, Evaluation of kinetic data for crystallization of TiO_2 prepared by hydrolysis method, J. Therm. Anal. Calorim. 60 (2000) 595–604.
[36] S. Liu, X. Chen, A visible light response TiO_2 photocatalyst realized by cationic S-doping and its application for phenol degradation, J. Hazard. Mater. 152 (2008) 48–55.
[37] Q. Zhang, L. Gao, One-step preparation of size-defined aggregates of TiO_2 nanocrystals with tuning of their phase and composition, J. Eur. Ceram. Soc. 26 (2006) 1535–1545.
[38] Y. Li, X. Sun, H. Li, S. Wang, Y. Wei, Preparation of anatase TiO_2 nanoparticles with high thermal stability and specific surface area by alcohothermal method, Powder Technol. 194 (2009) 149–152.
[39] S. Yin, H. Yamaki, M. Komatsu, Q. Zhang, J. Wang, Q. Tang, F. Saito, T. Sato, Preparation of nitrogen-doped titania with high visible light induced photocatalytic activity by mechanochemical reaction of titania and hexamethylenetetramine, J. Mater. Chem. 13 (2003) 2996–3001.
[40] B. Sun, P.G. Smirniotis, P. Boolchand, Visible light photocatalysis with platinized rutile TiO_2 for aqueous organic oxidation, Langmuir 21 (2005) 11397–11403.
[41] S.X. Liu, X.Y. Chen, X. Chen, A TiO_2/AC composite photocatalyst with high activity and easy separation prepared by a hydrothermal method, J. Hazard. Mater. 143 (2007) 257–263.
[42] J.-P. Meng, J.-S. Liang, G.-C. Liang, J.-M. Yu, Y.-F. Pan, Effects of tourmaline on microstructures and photocatalytic activity of TiO_2/SiO_2 composite powders, Trans. Nonferrous Metals Soc. China 16 (2006) s547–s550.
[43] J.M. Herrmann, Heterogeneous photocatalysis: fundamentals and applications to the removal of various types of aqueous pollutants, Catal. Today 53 (1999) 115–129.
[44] C.-H. Wu, C.-H. Yu, Effects of TiO_2 dosage, pH and temperature on decolorization of C.I. Reactive Red 2 in a UV/US/TiO_2 system, J. Hazard. Mater. 169 (2009) 1179–1183.